Monte Carlo Simulation of Massive Absorbers for Cryogenic Calorimeters

Citation: Brandt, D. et al. "Monte Carlo Simulation of Massive Absorbers for Cryogenic Calorimeters." Journal of Low Temperature Physics 167.3–4 (2012): 485–490.

As Published: http://dx.doi.org/10.1007/s10909-012-0480-3

Publisher: Springer US

Persistent URL: http://hdl.handle.net/1721.1/105501

Version: Author's final manuscript: final author's manuscript post peer review, without publisher's formatting or copy editing

J Low Temp Phys (2012) 167:485–490
DOI 10.1007/s10909-012-0480-3

Monte Carlo Simulation of Massive Absorbers for Cryogenic Calorimeters

D. Brandt · M. Asai · P.L. Brink · B. Cabrera · E. do Couto e Silva · M. Kelsey · S.W. Leman · K. McArthy · R. Resch · D. Wright · E. Figueroa-Feliciano

Received: 9 August 2011 / Accepted: 3 January 2012 / Published online: 9 February 2012

Abstract There is a growing interest in cryogenic calorimeters with macroscopic absorbers for applications such as dark matter direct detection and rare event search experiments. The physics of energy transport in calorimeters with absorber masses exceeding several grams is made complex by the anisotropic nature of the absorber crystals as well as the changing mean free paths as phonons decay to progressively lower energies. We present a Monte Carlo model capable of simulating anisotropic phonon transport in cryogenic crystals. We have initiated the validation process and discuss the level of agreement between our simulation and experimental results reported in the literature, focusing on heat pulse propagation in germanium. The simulation framework is implemented using Geant4, a toolkit originally developed for high-energy physics Monte Carlo simulations. Geant4 has also been used for nuclear and accelerator physics, and applications in medical and space sciences. We believe that our current work may open up new avenues for applications in material science and condensed matter physics.

Keywords Phonons · Cryogenic calorimeter · Monte Carlo · Germanium · Geant4 · CDMS

D. Brandt (✉) · M. Asai · P.L. Brink · E. do Couto e Silva · M. Kelsey · R. Resch · D. Wright
SLAC National Accelerator Laboratory, Menlo Park, CA 94025, USA
e-mail: dbrandt@slac.stanford.edu

B. Cabrera
Stanford University, Palo Alto, CA 94305, USA

S.W. Leman · K. McArthy · E. Figueroa-Feliciano
MIT, Cambridge, MA 02139, USA

1 Introduction

Cryogenic calorimeters can provide excellent energy resolution in a very low noise environment [1]. In recent years there has been a growing interest in exploiting the high energy resolution and good noise characteristics of cryogenic calorimeters in dark matter direct detection experiments [2–4] and other rare event searches [5]. Typically, a macroscopic absorber with mass of order *hundreds of grams*, is instrumented with a large number of cryogenically cooled thermometers in order to detect energy deposited in the crystal in the form of athermal phonons. The Cryogenic Dark Matter Search (CDMS) which provided the motivation for the work presented here uses a large semiconductor absorber with thousands of Transition Edge Sensor (TES) thermometers sputtered onto the crystal surface [6].

The physics of energy transport in cryogenic absorbers is non-trivial. Phonon transport is highly anisotropic [7, 8] and the spontaneous decay of high energy into low energy phonons leads to a rapidly evolving characteristic mean free path of the phonon system. The propagation behaviour of the downconverting phonons changes from diffuse scattering, with mean free paths of order microns, to the ballistic regime, with mean free paths comparable to the crystal dimension [9, 10]. This quasidiffuse propagation behaviour makes the analytical treatment of phonon propagation in the absorber highly problematic. Monte Carlo simulation is a suitable tool for numerically studying the evolution of the phonon system [10].

Here we present our efforts to develop a Monte Carlo simulation framework capable of capturing phonon transport physics in cryogenic absorbers. The framework simulates phonon scattering of isotopic impurities ("isotope scattering"), changes in phonon polarization state during scattering events ("mode mixing") and the anharmonic decay of high energy phonons ("downconversion"). The framework is implemented using the Geant4 toolkit. Geant4 is a C++ based toolkit for the simulation of particle transport through matter [11]. It is available under a public license and offers a great amount of flexibility in setting up complex simulation geometries. The Monte Carlo model described in this paper constitutes the first solid state physics framework for Geant4.

Our efforts to implement a Monte Carlo simulation of energy transport in cryogenic crystals are motivated by the Cryogenic Dark Matter Search (CDMS) experiment, which uses cryogenic detectors with large (≈1 kg) Germanium absorbers [6]. Hence, examples and validation of simulated quantities discussed use Germanium crystal absorbers. However, we believe that the flexibility of the Geant4 toolkit will allow other experiments to benefit from the phonon transport code discussed here.

2 Phonon Physics

In this section the phonon propagation physics of the simulation framework are discussed. Section 2.1 discusses the implementation of anisotropic phonon transport and phonon focusing in elastic crystals. Section 2.2 discusses the implementation of isotope scattering and downconversion processes used to evolve the phonon distribution.

2.1 Anisotropic Phonon Propagation

Phonon propagation in the absorber crystal is governed by the three-dimensional wave equation [12]:

$$\rho\omega^2 e_i = C_{ijlm} k_j k_m e_l \tag{1}$$

where ρ is the crystal mass density, ω is the phonon frequency, $\mathbf{e}$ is the polarization vector, $\mathbf{k}$ is the wave vector and $\mathbf{C}_{ijml}$ is the elasticity tensor.

By solving (1) for a phonon of given wave vector $\mathbf{k}$, three eigenvalues ω and three eigenvectors $\mathbf{e}$ can be found, corresponding to three discrete polarization states *Longitudinal (L), Fast Transverse (FT)*, and *Slow Transverse (ST)*.

In the crystal energy transport occurs along the group velocity vector $\mathbf{v_g}$, which can be found from (1) as

$$\mathbf{v_g} = \frac{d\omega(\mathbf{k})}{d\mathbf{k}} = \nabla_k \omega(\mathbf{k}) \tag{2}$$

A detailed discussion regarding methods for solving the wave equation (1) and recovering the group velocity vector $\mathbf{v_g}$ can be found in Wolfe [12]. There are two key aspects to the solution of the wave equation:

1. The momentum vector $\hbar\mathbf{k}$ is not generally parallel to the vector of energy transport $\mathbf{v_g}$. Phonons are focussed along preferred directions of propagation in the crystal. This effect is known as "Phonon focusing" and discussed in great detail by Wolfe [12] and Nothrop and Wolfe [8].
2. Phonons at frequencies characteristic of quasi diffusion are non-dispersive. Hence, the phonon phase velocity ω/k and group velocity $d\omega/dk$ are independent of angular frequency ω. For a given crystal $\mathbf{v_g}$ is a function of phonon direction $\mathbf{k}/k$ only [12, 13].

In the simulation framework, (1), (2) are not solved in real time. Instead, a set of maps is pre-built and loaded at runtime to map phonon wave vectors $\mathbf{k}$ onto group velocities $\mathbf{v_g}$.

The elasticity tensor elements C_{ijml} for various commonly used crystals are given by Wolfe [12].

2.2 Phonon Processes

The phonon system is evolved by elastic and inelastic scattering events. Elastic scattering typically occurs at isotope substitution sites and is therefore called isotope scattering. The isotropic isotope scattering rate $\Gamma_{scatter}$ is given by [10]:

$$\Gamma_{scatter} = B\nu^4 \tag{3}$$

where $\nu = E_{ph}/h$ is the phonon frequency, E_{ph} is the phonon energy and B is a constant derived from the crystal elasticity tensor. The derivation of B and the elasticity tensor components necessary to calculate it are given by (11) and Table 1 in Tamura [13].We find $B = 3.67 \times 10^{-41}$ s^3 [13].

As a phonon undergoes isotope scattering, its wave vector k is randomized. In the simulation, the branching ratio is approximated as isotropic and equal to the ratio of

density of states of L, FT, ST modes. The full isotropic and anisotropic treatment of isotope scattering and the relevant branching ratio is given by Tamura [10].

In inelastic scattering events, energetic phonons spontaneously decay into pairs of less energetic phonons. This process is known as anharmonic decay and results from anharmonic terms in the elastic response of the crystal [9, 10]. In general, all phonon types can downconvert but transverse phonon decay rates are so small as to be negligible compared to longitudinal phonon decay rates [10]. The bulk rate of L-phonon downconversion Γ_{anh} is given by [10]

$$\Gamma_{anh} = A\nu^5 \tag{4}$$

where $\nu = E_{ph}/h$ is the phonon frequency and A is a constant derived from the crystal elasticity tensor. The derivation of A and the elasticity tensor components necessary to calculate it are given by (11) and Table 1 in Tamura [13]. For Ge we find [13] $A = 6.43 \times 10^{-55}$ s^4.

Following an anharmonic decay event, the wave vector directions of the daughter phonons are determined by assuming that the group velocity is isotropic and requiring that energy and momentum are conserved. Thus if a phonon of wave-vector k decays into a phonon pair of wave-vectors k', k'' the daughter wave-vectors are determined from the relationship $k = k' + k''$. The energy partitioning between daughter phonons has been determined according to the expressions given by Tamura [10].

3 Validating the Geant4 Implementation

Experimental phonon focusing patterns resulting from anisotropic propagation effects discussed in Sect. 2.1 have been recorded experimentally using heat pulse excitation of ballistic phonons [8, 13].

The right-hand panel in Fig. 1 shows an observed intensity pattern in Ge reported by Nothrop and Wolfe [8]. The left-hand panel shows an intensity pattern generated using the Geant4 phonon transport code. It can be seen that the simulation reproduces the caustic features observed by experiment. The additional features shown in the simulated caustic are predicted to exist in the experimental system as well [8], however, it seems that their intensity was too low to be observed.

All propagation directions and velocities in the simulation are derived from the elasticity tensor $\mathbf{C}_{ijml}$ using the three dimensional wave equation (1). Hence, an important part of the validation process is a comparison of the phonon flux timing histogram for a heat pulse propagating through the crystal.

Nothrop and Wolfe have initiated a heat pulse on one face of a small (1 cm^3) Ge crystal using a pulsed Nd:YAG laser and recorded a timing histogram of the phonon flux incident on the opposite crystal face using a cryogenic bolometer [8]. An identical setup has been modeled using the Geant4 phonon transport code. The observed and simulated timing histograms of the heat pulse propagation through the crystal are shown in Fig. 2. It can be seen that the phonon flux arrives in three separate pulses, corresponding to the three phonon polarization states. It can be seen that the time delays between the three simulated polarization peaks is in good agreement with experimental data. Both simulated and experimental polarization peaks have a similar

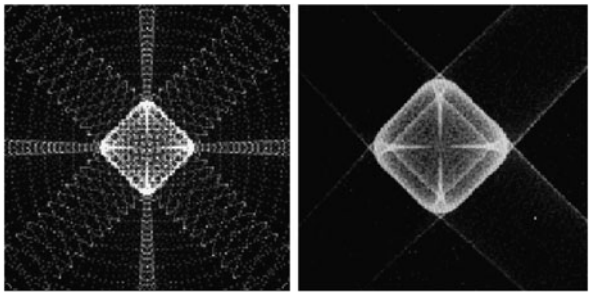

Fig. 1 Caustic intensity pattern generated by the heat pulse experiment. *Left*: as simulated by the Geant4 phonon transport code. *Right*: as reported by Nothrop and Wolfe [8].The field of view is approximately 30° from the [100] crystal axis

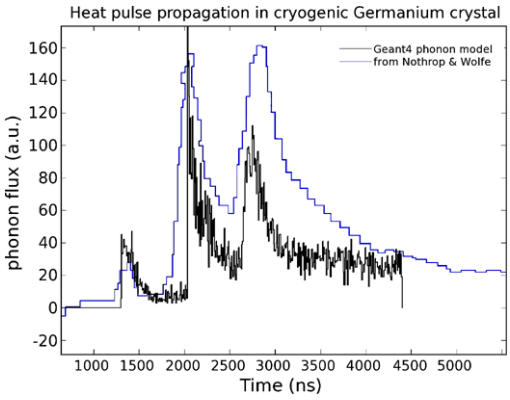

Fig. 2 (Color online) Phonon flux timing histogram of the heat pulse experiment. The figure shows experimental data according to Nothrop and Wolfe [8] (coarse histogram) and a phonon pulse simulated using the Geant4 phonon transport code

qualitative peak profile comprising a steep rising edge followed by a much longer fall time.

In order to obtain the simulated histogram in Fig. 2 the Germanium crystal was assumed to be cubic, with the bolometer in the (011) plane of the crystal. Since no precise dimensions were given for the Germanium crystal investigated experimentally by Nothrop and Wolfe [8], the crystal side length was inferred from the time delay between the leading edges of the L- and ST-peaks to be approximately 7.2 mm. In the simulation, the initial spectrum of phonons created by the laser pulse was assumed to follow a $T = 20$ K Planckian distribution, with all phonons created at a point 1 μm inside the crystal (corresponding to the decay length of the $\lambda = 1.06$ μm laser used in the experiment [8]) and at the center of the crystal face.

A small time delay can be seen in Fig. 2 between the leading edge of the simulated pulses and the leading edge of the timing histogram as observed by Nothrop and Wolfe [12]. We believe that the most likely reason for this delay is that the laser pulse used to excite the phonons had a width of ≈200 ns in the experiment [8] while all simulated phonons are excited at time $t = 0$. It is not entirely clear how $t = 0$ was defined in the experiment by Nothrop and Wolfe, but it appears that it may have been set to the time of laser pulse peak power rather than the onset of the pulse. The region of phonon emission was simulated as a point source, rather than as a three dimensional volume, and contributions from electron-hole pair creation and recombination have not been considered.

4 Conclusions

A phonon transport code has been implemented using the Geant4 C++ toolkit. The transport code succesfully uses pre-calculated maps to simulate anisotropic phonon propagation and phonon focusing in Germanium crystals as demonstrated by the good qualitative agreement between simulated and observed phonon caustics. Timing histograms of heat pulse propagation experiments in small Ge crystals are reproduced with some qualitative agreement, demonstrating the transport code's ability to model and reproduce simple experimental geometries. Small timing discrepancies between simulated and observed data are likely due to uncertainties about experimental heating pulse onset and time length. Further improvements in agreement may be possible by taking into account excitation and recombination of electron-hole pairs [8].

The phonon transport code discussed in this paper represents the first condensed matter framework for Geant4. Given the free availability and enormous flexibility of the Geant4 system to model complex geometries, the phonon transport code should be applicable in principle to any cryogenic calorimeter experiment with non-metallic crystal absorbers (i.e. insulator or semiconductor), provided the required crystal elasticity tensor is known. In order to make the transport code more universally applicable, an effort is underway to include drifting electron-hole pairs in the simulation, as well as phonon excitation by accelerated charge carriers.

Acknowledgements We would like to acknowledge the support of the CDMS Detector Monte Carlo simulation team. Additional work regarding the Monte Carlo simulation of energy transport in cryogenic semiconductor crystals and particularly the CDMS detectors can be found in the contributions by Leman [14], McCarthy [15] and Anderson [16]. This work was supported in part by the Department of Energy contract DE-AC02-76SF00515 under the SLAC National Accelerator Lab LDRD program.

References

1. C. Enss, *Cryogenic Particle Detection* (Springer, Berlin, 2005)
2. Z. Ahmed et al., Science **327**, 1619 (2010)
3. V. Sanglard et al., Phys. Rev. D **71**, 122002 (2005)
4. R.F. Lang, W. Seidel, New J. Phys **11**, 105017 (2009)
5. C. Arnaboldi et al., Nucl. Instrum. Methods A **3**, 775 (2004)
6. P. Brink et al., Nucl. Instrum. Methods A **2**, 414 (2006)
7. D.C. Hurley, J.P. Wolfe, Phys. Rev. B **32**, 2568 (1985)
8. G.A. Nothrop, J.P. Wolfe, Phys. Rev. Lett. **19**, 1424 (1979)
9. S. Tamura, J. Low Temp. Phys. **93**, 433 (1993)
10. S. Tamura, Phys. Rev. B **48**, 13502 (1993)
11. J. Allison et al., IEEE Trans. Nucl. Sci. **1**, 270 (2006)
12. J.P. Wolfe, *Imaging Phonons* (Cambridge University Press, Cambridge, 1998) Chap. 2, 42
13. S. Tamura, Phys. Rev. B. **31** (1985)
14. S.W. Leman et al., J. Low Temp. Phys. (2012). doi:10.1007/s10909-012-0465-2
15. K.A. McCarthy et al., J. Low Temp. Phys. (2012). doi:10.1007/s10909-012-0474-1
16. A. Anderson et al., J. Low Temp. Phys. (2012). doi:10.1007/s10909-012-0555-1